arXiv:1512.05417v2 [cs.SI] 2 Mar 2016

Influence Prediction for Continuous-Time Information Propagation on Networks

Shui-Nee Chow, Xiaojing Ye, Hongyuan Zha, Haomin Zhou *

Abstract

We consider the problem of predicting the time evolution of influence, the expected number of activated nodes, given a set of initially active nodes on a propagation network. To address the significant computational challenges of this problem on large-scale heterogeneous networks, we establish a system of differential equations governing the dynamics of probability mass functions on the state graph where the nodes each lumps a number of activation states of the network, which can be considered as an analogue to the Fokker-Planck equation in continuous space. We provides several methods to estimate the system parameters which depend on the identities of the initially active nodes, network topology, and activation rates etc. The influence is then estimated by the solution of such a system of differential equations. This approach gives rise to a class of novel and scalable algorithms that work effectively for large-scale and dense networks. Numerical results are provided to show the very promising performance in terms of prediction accuracy and computational efficiency of this approach.

1 Introduction

Viral signal propagation on networks is an emerging research subject of both theoretical and practical importance. The problem of estimating the influence of propagation arises from several applications of significant societal impact, such as news spread on social media, viral marketing, computer malware detection, and epidemics of infectious diseases on large-scale heterogeneous networks. For instance, when considering a social network formed by people such as that of Facebook or Twitter, the viral signal can be a tweet on a trendy topic being retweeted by users on the network. A viral signal can also be a new electronic gadget that finds wide-spread adoption in the user population through a word-of-mouth viral marketing process [36, 37, 51]. To this end, an important question is how to predict the influence, defined by the expected number of nodes activated during the propagation of any given initial source set of activated nodes, whereby node activation can mean retweeting of a tweets or adoption of a gadget by a user. Moreover, solutions to several important downstream applications such as influence maximization [10, 28, 31, 61] and outbreak detection [11, 37] problems also rely on effective influence prediction for any specific combination of initially active nodes in a given network. For instance, in influence maximization, the goal is to select the

*S.-N. Chow and H.-M. Zhou are with School of Mathematics, Georgia Institute of Technology, Atlanta, GA 30332, USA, X. Ye is with Department of Mathematics & Statistics, Georgia State Univeristy, Atlanta, GA 30303, USA, and H. Zha is with Computational Science & Engineering, College of Computing, Georgia Institute of Technology, Atlanta, GA 30332, USA. Emails: {chow,hmzhou}@math.gatech.edu, xye@gsu.edu, zha@cc.gatech.edu. This work is supported in part by NSF DMS-1317424, DMS-1419027, NIH R01 GM108341, and ONR Award N000141310408.

source node set of a given size from the propagation network such that its influence is maximized at a prescribed time. Therefore, influence prediction serves as the most fundamental subroutine in this process.

1.1 Problem description

The influence prediction problem can be formulated as follows. Let $G(V, E)$ be a given network (directed graph, we use network and graph interchangeably in this paper) with node set $V = \{i : 1 \leq i \leq K\}$ and edge set E. The node i is called a parent of j, or j a child of i, if there is a directed edge from i to j, denoted by $(i, j) \in E$. In this paper, we use $D_i = \{j : (j, i) \in E\}$ to denote the parent set of i, and $C_i = \{j : (i, j) \in E\}$ the child set of i. A piece of information on G can spread or propagate from an active node i to every inactive $j \in C_i$, and once succeeded, node j becomes active and starts to propagate information to its child in C_j, and so on. In addition to node-to-node activations, the nodes may also have the ability of self-activation or recovery (i.e., becoming inactive, more relevant in the infectious disease case), or both. In the self-activation scenario, an inactive node i can be self-activated regardless whether it has active parents or not. On the other hand, in the recovery scenario, an active node i may recover and become inactive. The nodes thus have binary states: either inactive (susceptible) or active (infected). With recovery scenario, the activation model is also called the susceptible-infected-susceptible (SIS) model, otherwise it simplifies to the susceptible-infected (SI) model.

In real world applications, the propagation usually exhibits randomness as it is uncertain whether or when an active parent activates its children, or a node becomes self-activated or recovered. Here we adopt an approach to model the dynamics of network information propagation as continuous-time stochastic processes.

Given the network $G(V, E)$, the stochastic propagation process is determined by the distribution of the activation times between nodes. In this paper, we assume that the time for i to activate each j, denoted by $t_{i,j}$, follows $\exp(\alpha_{i,j})$ distribution[1] and is independent of any other $t_{i',j'}$ where $i \neq i'$ and/or $j \neq j'$. Here $\alpha_{i,j} > 0$ indicates the instantaneous activation rate of j by i. If $(i, j) \notin E$, we set $\alpha_{i,j} = 0$ by convention. Note that exponential random variable following $\exp(\alpha)$ has mean $1/\alpha$, therefore, the larger $\alpha_{i,j}$ is, the faster i can activate j on average. Hence $\alpha_{i,j}$ can be interpreted as the degree of impact (weight) of i on j.

The continuous-time propagation model with heterogeneous activation rates appears suitable for a great number of real-world applications and has been advocated by many recent works [15, 28, 48, 58, 59]. In addition, this model yields a time-homogeneous Markov propagation process so that numerical simulations can be implemented in a straightforward manner and some theoretical analysis of the algorithm can be carried out. Therefore, we focus on the development of the algorithm on this propagation model, and evaluate the performance numerically to obtain references worthy of trust through a large amount of Monte Carlo simulations.

There are several ways to formulate the influence as the expected number of active nodes. First, let $X_i(t; S)$ be a binary variable such that $X_i(t; S) = 1$ if node i is active at time t and 0 otherwise, given the source set S of initially active nodes. Note that $\{X_i(t; S) : 1 \leq i \leq K\}$ are highly correlated stochastic processes. The influence $\mu(t; S)$ is then defined by the expectation of

[1] In this paper we call a nonnegative random variable t following $\exp(\alpha)$ distribution if the probability density function of t is $p_t(\tau) = \alpha e^{-\alpha\tau}$ for $\tau \geq 0$.

$\sum_i X_i(t;S)$ at time t:

$$\mu(t;S) = \mathrm{E}_{\{X_i:i\}}\left[\sum_{i\in V} X_i(t;S)\right] = \sum_{i\in V} \mathrm{E}_{X_i}\left[X_i(t;S)\right]. \tag{1}$$

Second, if there is no recovery, then one can also find the time $T_i(S)$ that each node i gets activated (which can occur at most once) given the source set S. Then $\{T_i(S) : 1 \le i \le K\}$ are dependent random variables, and $T_i(S) \le t$ if and only if $X_i(t;S) = 1$ for any $t > 0$. Therefore the influence can be defined by the following expectation in terms of $T_i(S)$:

$$\mu(t;S) = \mathrm{E}_{\{T_i:i\}}\left[|\{i \in V : T_i(S) \le t\}|\right]. \tag{2}$$

In the presence of recovery, each node i will have a sequence of change-of-status time points that determines if it is active by time t.

The third way, which we introduce and advocate here, is to define a single stochastic process $N(t;S)$ as the number of activated nodes at time t, namely

$$N(t;S) := \sum_{i\in V} X_i(t;S), \tag{3}$$

then directly compute the probability distribution of $N(t;S)$ defined as

$$\rho_k(t;S) := \mathrm{P}(N(t;S) = k), \quad \text{for } k = 0, 1, \ldots, K, \tag{4}$$

and obtain the influence by the expectation in terms of $N(t;S)$,

$$\mu(t;S) = \mathrm{E}_N[N(t;S)] = \sum_{k=0}^{K} k\rho_k(t;S), \tag{5}$$

where $K = |V|$ is the size of the network.

The main focus of this paper is to establish a general framework in the setting of the third approach based on (3) and (4). In particular, we build the system of equations for the time evolution of $\{\rho_k(t;S) : 0 \le k \le K\}$, analyze its properties, estimate the parameters in the equations, and solve for all $\rho_k(t;S)$ to predict the influence $\mu(t;S)$ in (5) for any given time t and source set S.

Remark 1. *It is worth pointing out that our new approach is based on the theory of mass transport and discrete Fokker-Planck equations. Note that the system of equations describing the evolution of $\{\rho_k(t;S) : 0 \le k \le K\}$ is analogous to the Fokker-Planck equation in the continuous space. To this end, let us recall that the classical Fokker-Planck equation, also known as the Kolmogorov forward equation, is a linear parabolic equation given by,*

$$\frac{\partial \rho(x,t)}{\partial t} = \nabla \cdot (\nabla \Psi(x)\rho(x,t)) + \beta \Delta \rho(x,t), \tag{6}$$

where $\Psi(x)$ is a given scalar-valued potential function, β a positive constant. $\Delta\rho(x,t)$ is called the diffusion term and $\nabla\cdot(\nabla\Psi(x)\rho(x,t))$ the drift term. It describes the time evolution of the probability density function ρ of a stochastic differential equation (SDE)

$$\mathrm{d}x = -\nabla\Psi(x)\,\mathrm{d}t + \sqrt{2\beta}\,\mathrm{d}W_t,\ x \in \mathbb{R}^n, \tag{7}$$

where W_t is the standard Brownian motion and $\mathrm{d}W_t$ is called the white noise. We remark that the Laplacian operator in (6) corresponds to the white noise term in (7). In fact, they are meant to describe diffusion from different perspectives.

In discrete settings, however, theoretical understandings on similar matters are very limited and different. For example, a recent study [9] shows that the Fokker-Planck equations on graphs must be systems of nonlinear ordinary differential equations, not a linear partial differential equation, if one wants to reach Gibbs distributions, the well known equilibrium of stochastic processes. The system of differential equations that we shall establish in this study is based on the Fokker-Planck equations on graphs which govern the time evolution of $\rho_k(t; S)$, the probability that the propagation network has k active nodes at time t given that the source set is S.

We emphasize that the proposed approach using discrete Fokker-Planck equation is a new framework that effectively exploits the random dynamics of the stochastic propagation process. Even though we only considered exponentially distributed activation times, it is a worthy future work to extend the current framework to other distribution models of the activation times. Our current paper addresses several technical problems arising from the new framework but at the same time it also raises a number of new open questions such as the approximation of the coefficients of the resulting Fokker-Planck equations and the associated error analysis for the approximation. We expect those to be tackled in the future research.

1.2 Related Work

Influence prediction is one of the most fundamental problems concerning information propagation, infectious disease, and viral marketing on large-scale networks. The computational challenges are mainly due to the randomness of propagation dynamics, varying activation rates between nodes, and heterogeneous topology of the large-scale networks.

In this section, we present a detailed overview of recent developments in several aspects closely related to the prediction of influence on propagation networks. A much more comprehensive treatment of the literature of dynamic systems on complex networks can be found in [7, 17, 46, 48, 50, 60] and the references therein. A large portion of current literature, especially in the context of dynamical systems on networks in statistical physics, deals with homogeneous or "well-mixed" populations where all nodes in the network are endowed with a certain degree distribution and handled equivalently. The goal of this paper, however, is to propose a new computational approach that effectively estimates influence of propagations on *heterogeneous networks of given connectivities and activation rates between nodes* based on discrete Fokker-Planck equations, where exact solution to such problem is generally considered computationally prohibitive in the literature.

Note that information propagation, as dynamic processes on networks, shares many common features with contagious epidemics, social networking, and flows on technological networks [33]. Therefore, we observe significant crossovers between the studies of these fields. In particular, Anderson and May provide a comprehensive summary of the developments in mathematical modeling of epidemics, and emphasize that heterogeneity plays an important role in disease spread [2]. The heterogeneity can be naturally modeled by structured networks that describe the interaction and contact between individuals [30, 46, 48, 60]. Therefore, the prediction of influence relies on the topological properties of the networks, the random dynamics of propagation, and the computational approaches for influence prediction.

1.2.1 Modeling real-world networks

The recent abundance of data and measurements of real-world networks implies a number of different network classes, characterized by a large variability in basic metrics and statistical properties. The widely used network generating models include the classical Erdős-Rényi random graphs described in [6, 18, 20, 13] where each of $K(K-1)$ edges has a prescribed probability $p \in (0,1)$ to be present, the small-world network model [64] that features both small diameter and large clustering coefficient, the scale-free networks where node degrees following power-law distribution [1, 3, 8, 47], and the more recent generative Kronecker network model [35].

The network models above are shown to exist in a variety of real-world network applications. There are parameters associate with these models that can be tuned to generate different size and topology for simulations. In our numerical experiment, we test our proposed method, along with several recently developed influence prediction algorithms, on these networks to verify their adaptability in various types of heterogeneous network structures.

1.2.2 Modeling stochastic propagation on networks

The modeling of information propagation on networks was originally studied by Durrett et al. [16] and Liggett [38] in particle interactions and later considered by Goldenberg et al. [23, 24] in the context of marketing. This study has triggered an extensive amount of work in a variety of economical and sociological research fields [19, 40, 41, 45, 49, 63, 66]. These works are mostly based on the node-specific threshold model, meaning that active parents can successfully activate a common child j if their total efforts (or weights) surpass the threshold specified by j in each time step [29, 31, 53].

In recent years, there are trends to model the activations as continuous-time processes. A continuous process accounts for temporally heterogeneous interactions between nodes and allows information spread at different rates, as in real-world applications [15, 25, 26, 27, 28, 48, 58, 59]. For instance, the time elapsed for i to activate j can be modeled as exponential distributions [48, 58, 59], Rayleigh distribution or general Weibull distributions [14, 15] with assumptions of independency between different activation processes and even Hawkes processes where nodes can be mutually excited with multiple concurrency [52, 68, 69]. As a consequence, the propagation can be interpreted as continuous-time stochastic processes on finite discrete-state spaces.

1.2.3 Influence prediction of propagation on networks

Given network topology and propagation model, one of the most fundamental problems on information propagation is the prediction of influence for a given source set of initially active nodes. As shown above, the influence describes on average how many nodes can be affected due to the source set during the course of propagation up to a certain time. In a given heterogeneous network, the influence of a given set of source nodes is determined by three key factors: the identities of these source nodes in S, the connectivities of the nodes in the network $G(V,E)$, and the activation/transmission rates $\{\alpha_{i,j} : (i,j) \in E\}$ (as well as self-activation β_i and recovery rates γ_i of nodes if the corresponding scenarios are considered).

There has been extensive work devoted to the study of influence estimation on networks with homogeneous and well-mixed populations, particularly in the context of statistical properties of dynamical processes on complex networks in physics. A typical approach is based on mean-field approximation (MFA) that establishes a system of differential equations for the probabilities of

activation of individual nodes. Then moment closure [43] is applied to approximate the joint distributions of activation states of adjacent nodes by ignoring correlations between them, and thus close the system [46, 48, 50]. Degree-based MFA groups nodes of the same degree which are considered to have identical behavior statistically, and hence can further reduce the size of the system [5]. Pair approximation includes the joint distribution in the system of equations, which essentially applies moment closure after the joint distribution of paired nodes, and is shown to have improved accuracy over MFA [4, 12, 46]. Moreover, Gleeson derived the approximate master equations for general stochastic binary-state dynamics which significantly improves the accuracy over degree-based MFA and pair approximation [21, 22]. Other generalization and improvements of MFA and pair approximation using compartment models and motif expansions can be found in [12, 39, 42, 43, 57].

For fixed heterogeneous networks, there are a number of works focusing on the limit of the influence as time tending to infinity, mostly in the context of stationary distribution or equilibrium of the stochastic process that describes the propagations [58, 59, 67]. However, it is often of great practical interests to estimate the time evolution of the influence especially in early to intermediate stage of the propagation, such as in viral marketing, disease spread, outbreak and contamination detection.

In [59], Van Mieghem et al. generalized the prototype MFA for Markov propagation model developed in [32, 62] to arbitrary network topology, and then further extended the work to inhomogeneous activation and recovery rate among nodes [58]. The model adopts the MFA and substitute the joint distribution to retain a feasible size of the resulting system of differential equations. Assuming absence of recovery, Gomez-Rodriguez et al. [28] showed that the problem can be solved exactly based on the shortest path method for Markov process on networks developed by Kulkarni [34]. However, the computational complexity of such approach increases exponentially with the size and density (the proportion of edges in the graph) of the general networks.

There are alternative approaches to predicting influence based on sampling and learning, which often pose various requirements on input data and output result. For instance, Du et al. developed a scalable method that learns the coverage function of each node based on sampling and kernel estimation, and it can only predict the influence at a prescribed time [15]. The work is further extended to estimate the time-varying intensity of propagation using similar coverage function idea [14]. Learning-based methods are usually companioned with a great amount of accuracy analysis based on classical theory of sampling complexity. However, the major problem with learning-based approaches is in the use of large amount of samplings to ensemble the unknown function or probability of interests but lack of a comprehensive understanding of the underlying dynamics and unique properties associated with the stochastic propagation on networks. Moreover, learning-based methods can have special assumptions on data which may not be realistic in real-world applications. For example, in disease spread on networks, it is often impossible to track down to the individuals who were the originals of infection and triggered the entire epidemic, however, the knowledge of their identities is required by the learning-based TCoverageLearner method [14]. Last but not least, to achieve moderate accuracy level in large-scale and complex network, learning-based methods require extensive amount of sampling/simulations which causes significant computational burden and hinders their applicability in real-world problems.

2 Proposed Method

In this section, we first provide several motivating examples using special graphs where the influence can be calculated easily and exactly using the proposed approach of discrete Fokker-Planck equations. Then we consider the system equations of (4) for general propagation networks, analyze their properties, and provide several methods to solve the system efficiently.

2.1 Several motivating examples and influence prediction

In these examples, we assume that all node-to-node activation rates are identical, denoted by α, and all nodes have the same self-activation rate β and recovery rate γ. We are interested in the time evolution of influence for any fixed source set S, and hence drop S for notational simplicity.

Example 2.1. *Undirected star graph $G(V, E)$ where $V = \{1, 2, \ldots, K\}$ and $E = \{(1, i), (i, 1) : i = 2, \ldots, K\}$. Namely, there is an undirected edge between the internal node indexed by 1 and every leave node indexed from 2 to K.*

Because of symmetry, we can denote every "metastate" by $[1, k]$ (a temporary abuse of bracket $[\,]$ notation) where the internal node and k leave nodes indexed between $\{2, \ldots, K\} \subset V$ are active, and $[0, k]$ if k leave nodes are active but internal node 1 is not. Therefore, in total there are $2(K-1)$ metastates of G, namely, $[1, k]$ and $[0, k]$ for $k = 0, 1, \ldots, K-1$. If we have the probability of the event $[0, k]$, denoted by $\rho_{[0,k]}(t)$, and $[1, k]$, denoted $\rho_{[1,k]}(t)$, at time t, then it is trivial to obtain the influence at time t by

$$\mu(t) = \sum_{k=0}^{K-1} \left(k\rho_{[0,k]}(t) + (k+1)\rho_{[1,k]}(t) \right). \tag{8}$$

Now let us turn to establishing the system of equations for $\rho_{[0,k]}(t)$ and $\rho_{[1,k]}(t)$, respectively, from which we can solve for these quantities. We note that if only k leave nodes are active in G, i.e. G is in metastate $[0, k]$, and each of those k nodes tends to recover at rate γ. Therefore, the instantaneous rate that G transits from $[0, k]$ to $[0, k-1]$ is $k\gamma$. Meanwhile, each of the $K-k-1$ inactive leave nodes also attempts for self-activation at rate β and hence the instantaneous rate from $[0, k]$ to $[0, k+1]$ is $(K-k-1)\beta$. Finally, the k active nodes are also trying to activate the internal node at rate α while the internal node is temping for self-activation at rate β, therefore the rate for G to turn from $[0, k]$ to $[1, k]$ is $k\alpha + \beta$. Similarly, the network at activation metastate $[1, k]$ can also transit to $[1, k-1]$, $[1, k+1]$, and $[0, k]$, with rates $k\gamma$, $(K-k-1)(\alpha+\beta)$, and γ, respectively. Now we are clear with all possible metastates to transit to from $[0, k]$ or $[0, k+1]$, and the associated rates. Therefore, we can establish a system of differential equations of $\rho_{[0,k]}(t)$ and $\rho_{[1,k]}(t)$ as follows,

$$\begin{aligned}
\rho'_{[0,k]} &= (K-k)\beta\rho_{[0,k-1]} + \gamma\rho_{[1,k]} + (k+1)\gamma\rho_{[0,k+1]} \\
&\quad - (k(\alpha+\gamma) + (K-k)\beta)\rho_{[0,k]}, \\
\rho'_{[1,k]} &= (K-k)(\alpha+\beta)\rho_{[1,k-1]} + (k\alpha+\beta)\rho_{[0,k]} + (k+1)\gamma\rho_{[1,k+1]} \\
&\quad - ((K-k-1)(\alpha+\beta) + (k+1)\gamma)\rho_{[1,k]},
\end{aligned} \tag{9}$$

for all $k = 0, 1, \ldots, K-1$. Note that this is a linear system of size $2K$, and its solution can be readily obtained by computing matrix exponentials.

The analysis above can be readily generalized to complete bipartite graphs $G(V, E)$ where $E = \{(i, j), (j, i) : 1 \le i \le L, L + 1 \le j \le K\}$, i.e., there are L nodes in one partition and $K - L$ in the other. In this case, one can construct a linear system of size $(L + 1)(K - L + 1) \le O(K^2)$.

Example 2.2. *Undirected complete graph $G(V, E)$ where $V = \{1, \ldots, K\}$ and $E = \{(i, j) : 1 \le i, j \le K\}$.*

In this case, there are $K + 1$ metastates where $N(t)$ defined in (3) is k for $k = 0, 1, \ldots, K$. Now we establish the system of $\rho_k(t)$ defined in (4), and use the solution of this system to compute $\mu(t)$ according to (5).

We note that the network with k active nodes can transit to the metastate of $k-1$ active nodes at rate $k\gamma$ since each of the k active nodes is recovering at rate γ. On the other hand, the network may also transit to the metastate of $k + 1$ active nodes at rate $k(K - k)\alpha + (K - k)\beta$, since each of the $K - k$ inactive nodes can be activated by any of the k active nodes at rate α or by itself at rate β. Therefore

$$\begin{aligned} \rho_k' = &((k-1)(K-k+1)\alpha + (K-k+1)\beta)\,\rho_{k-1} \\ &- (k(K-k)\alpha + (K-k)\beta + k\gamma)\,\rho_k + (k+1)\gamma\rho_{k+1} \end{aligned} \tag{10}$$

for $k = 0, 1, \ldots, K$ with $\rho_{-1} = \rho_{K+1} = 0$ by convention.

We point out here that the resulting system is of size $K+1$. Specifically, let $\rho(t) = (\rho_0(t), \rho_1(t), \ldots, \rho_K(t))$, then the linear system can be simply written as

$$\rho'(t) = \rho(t)Q \tag{11}$$

where the generator matrix $Q = [Q_{k,l}]$ is a $(K + 1)$-by-$(K + 1)$ tridiagonal (bidiagonal if $\gamma = 0$) matrix with diagonal, superdiagonal, and subdiagonal entries as

$$\begin{aligned} Q_{k,k} &= -[k(K-k)\alpha + (K-k)\beta + k\gamma] \\ Q_{k,k+1} &= k(K-k)\alpha + (K-k)\beta \\ Q_{k,k-1} &= k\gamma \end{aligned} \tag{12}$$

for $k = 0, 1, \ldots, K$ with convention $Q_{0,-1} = 0, Q_{K,K+1} = 0$. Hence, the solution can be easily obtained by

$$\rho(t) = \rho(0)e^{tQ} \tag{13}$$

where the $|S|$-th component of the initial value $\rho(0)$ is 1 and other components are 0.

Note that the solution described by (13) is exact, and computational complexity is very low because of the linear growth of system size as K increases and simple tridiagonal structure of Q. The appendix continues the discussion on the property of such network in terms of the stationary distribution revealed by the eigen-system of Q. We remark that, for this specific example with homogeneous network structure and activation rates, existing methods such as approximate master equation [21] can also provide exact solution efficiently. However, as we show in the next section, the proposed approach using Fokker-Planck equations establishes a new framework that can also tackle the influence prediction problem on general heterogeneous networks.

2.2 The general case

From the examples above, we can see that influence prediction problem can be effectively tackled by studying the time evolution of probability distribution of $N(t)$. In this case, the system is written as

$$\begin{aligned}\rho_k'(t) = q_{k-1}(t, \rho_{[0,t)})\rho_{k-1}(t) - [q_k(t, \rho_{[0,t)}) + r_k(t, \rho_{[0,t)})]\rho_k(t) \\ + r_{k+1}(t, \rho_{[0,t)})\rho_{k+1}(t)\end{aligned} \tag{14}$$

where $k = 0, 1, \ldots, K$ with the convention $\rho_{-1}(t) = \rho_{K+1}(t) = 0$. Here $\rho_{[0,t)}$ is the history of ρ during time $[0, t)$, and $q_k(t, \rho_{[0,t)})$ represents the instantaneous hazard rate for the $(k+1)$-th node to get activated at time t and $r_k(t, \rho_{[0,t)})$ is the instantaneous reversing rate for one of the active k nodes to recover, which may depend on both t and $\rho_{[0,t)}$. The analytic form for those functions is not readily available in general, nevertheless, Equation (14) is consistent with the nature of stochastic process $N(t)$ and results in a system of history dependent differential equations as $\rho'(t) = \rho(t)Q(t, \rho_{[0,t)})$. Here Q has a similar tridiagonal structure as in (12), but with q_k, $-(q_k + r_k)$, and r_k as the superdiagonal $Q_{k,k+1}$, diagonal $Q_{k,k}$, and subdiagonal $Q_{k,k-1}$ entries of matrix Q, respectively. The states and transitions are illustrated in (15), where M_k stands for the metastate of G with exactly k active nodes for $k = 0, 1, \ldots, K$.

$$\boxed{M_0} \rightleftharpoons \cdots \rightleftharpoons \boxed{M_{k-1}} \underset{r_k}{\overset{q_{k-1}}{\rightleftharpoons}} \boxed{M_k} \underset{r_{k+1}}{\overset{q_k}{\rightleftharpoons}} \boxed{M_{k+1}} \rightleftharpoons \cdots \rightleftharpoons \boxed{M_K} \tag{15}$$

In summary, the propagation on G yields a continuous-time stochastic process on the chain of metastates $\{M_k : 0 \le k \le K\}$ illustrated by (15), where the evolution of metastate probabilities $\rho_k(t)$ is a system of differential equations of form (14) with q_k and r_k to be determined. This system of ordinary differential equations is an analogue to the Fokker-Planck equations in the continuous case, and q_k and r_k measure the transition rates of probability mass $\{\rho_k : 0 \le k \le K\}$ between the metastates. In a similar spirit of the Fokker-Planck equation (6) in continuous case, the system (14) establishes the evolution of $\rho_k(t)$ on the discrete states M_k where these rates q_k and r_k, determined by the propagation dynamics on the network, can be thought of as the driven force that causes the temporal changes of the probability mass.

2.3 Estimation of instantaneous transition rates

As we can see from (14), the key to obtaining the evolving probability $\rho(t)$ is estimating the instantaneous hazard rate $q_k(t, \rho_{[0,t)})$ and reversing rate $r_k(t, \rho_{[0,t)})$. We have calculated these rates in the complete graph example in (12) which turn to be constant. In general, however, an analytic formulation of these rates in terms of t and ρ is intractable. Therefore, we propose several methods to approximate these rates and discuss their properties and computational complexity. The practical performance of these methods are shown in the numerical experiment section.

First of all, we emphasize the interpretation of q_k that it stands for the instantaneous rate for the k currently active nodes to activate any of the remaining $K - k$ inactive nodes. Similarly, r_k is the instantaneous rate that for any of the k active nodes recovers. The rate q_k consists of two factors: (i) the specific combination of the k active nodes and (ii) the instantaneous hazard rate they impose at the time. In terms of instantaneous hazard rate $\alpha(t; i_1, \ldots, i_k)$ in (ii), we meant that

$$\alpha(t; i_1, \ldots, i_k) := \lim_{\Delta t \to 0^+} \frac{1}{\Delta t} \mathrm{E}\left[N(t + \Delta t | i_1, \cdots, i_k) - N(t | i_1, \cdots, i_k)\right] \tag{16}$$

and $N(t|i_1, \cdots, i_k)$ is the event (a successful activation is considered as one event) counting process at time t given that $i_1, \ldots, i_k$ are active at the moment. The instantaneous recovery rate r_k can be defined in a similar way, except that the event is a recovery of an active node. For the Markov model considered in this paper, the instantaneous hazard rate and recovery rate for a given fixed combination of nodes are constant and easy to obtain, as we show in the theorem below. In terms of (i), we realize that in general there are as many as $\binom{K}{k}$ possible combinations to specify the k active nodes in a propagation network of size K at any moment. If we have the probability of every combination $(i_1, \ldots, i_k)$ at time t, denoted by $\mathrm{P}(t; i_1, \ldots, i_k)$, then the instantaneous rates q_k and r_k can be easily constructed, according to the theorem below.

To prepare the justification of our claim, we start with a basic fact about independent exponentially distributed random variables. The following proposition states that, when multiple activations (whose times are exponentially distributed) occur simultaneously and independently, the time of first success is also exponentially distributed, and the probability that one of them is minimum is proportional to their weights. The proof of this proposition is simple and can be found in a variety of textbooks, and hence is omitted here.

Proposition 2.1. *Let $T_1, T_2, \ldots, T_n$ be independent random variables and $T_i \sim \exp(\alpha_i)$ for $i = 1, \ldots, n$, then the probability that $T_i = \min\{T_j : 1 \le j \le n\}$ is*

$$\mathrm{P}(T_i \le T_j,\ \forall j) = \frac{\alpha_i}{\sum_{i'=1}^{n} \alpha_{i'}}, \tag{17}$$

and the minimum $\min\{T_i : 1 \le i \le n\} \sim \exp(\sum_{i=1}^{n} \alpha_i)$.

Recall that the instantaneous rates q_k and r_k depend on the specific combination of k active nodes and the combined hazard/recovery rate these k nodes generate. The following lemma exploits these rates in a general setting, which explains how q_k and r_k are constituted.

Lemma 2.1. *Let $T_i \sim \exp(\alpha_i)$ and Y be a multinomial random variable such that $\mathrm{P}(Y = i) = p_i$ for $i = 1, \ldots, n$, then the probability density function of T_Y is*

$$f_{T_Y}(t) = \sum_{i=1}^{n} p_i \alpha_i e^{-\alpha_i t}, \tag{18}$$

and the instantaneous hazard rate of point process associated to time T_Y is

$$\alpha_{T_Y}(t) = \frac{\sum_{i=1}^{n} p_i \alpha_i e^{-\alpha_i t}}{\sum_{i=1}^{n} p_i e^{-\alpha_i t}}. \tag{19}$$

In particular, $\alpha_{T_Y}(0) = \sum_{i=1}^{n} p_i \alpha_i$.

Proof. We use the rule of total probability to obtain

$$\mathrm{P}(T_Y \ge t) = \sum_{i=1}^{n} \mathrm{P}(T_Y \ge t | Y = i)\, \mathrm{P}(Y = i) = \sum_{i=1}^{n} p_i e^{-\alpha_i t}. \tag{20}$$

Hence the cumulative distribution function of T_Y is $F_{T_Y}(t) = 1 - \mathrm{P}(T_Y \ge t)$ and probability density function is $f_{T_Y}(t) = F'_{T_Y}(t) = \sum_{i=1}^{n} p_i \alpha_i e^{-\alpha_i t}$. The instantaneous hazard rate is then given by $\alpha_{T_Y}(t) = f_{T_Y}(t) / \mathrm{P}(T_Y \ge t)$. □

In light of Lemma 2.1, we have the following theorem that reveals the constitutions of rates q_k and r_k.

Theorem 2.1. *For each of $k = 0, 1, \ldots, K$, let $\mathrm{P}(t; i_1, \ldots, i_k)$ be the probability that nodes $i_1, \ldots, i_k$ form the combination of k active nodes in G at time t, then the instantaneous rates in (14) are given by*

$$q_k(t) = \sum_{(i_1,\ldots,i_k)\subset V} \left(\alpha(i_1, \ldots, i_k) + \sum_{j\neq i_l, \forall l} \beta_j \right) \mathrm{P}(t; i_1, \ldots, i_k), \tag{21}$$

$$r_k(t) = \sum_{(i_1,\ldots,i_k)\subset V} \left(\sum_{l=1}^{k} \gamma_{i_l} \right) \mathrm{P}(t; i_1, \ldots, i_k), \tag{22}$$

where the combined hazard rate $\alpha(i_1, \ldots, i_k)$ of active nodes $\{i_1, \ldots, i_k\}$ is given by

$$\alpha(i_1, \ldots, i_k) := \sum_{l=1}^{k} \sum_{j\in C_{i_l}\setminus\{i_1,\ldots,i_k\}} \alpha_{i_l,j}. \tag{23}$$

Proof. Note that for propagation network G to be in metastate M_k as shown in (14), there are exactly k active nodes in G. In total there are $\binom{K}{k}$ possible combinations of k nodes from network G of size K at any time t. If the probability of each combination $\{i_1, \ldots, i_k\}$ is $\mathrm{P}(t; i_1, \ldots, i_k)$, we just need to find the combined instantaneous hazard and recovery rates of $\{i_1, \ldots, i_k\}$ according to Lemma 2.1.

Suppose nodes $i_1, \ldots, i_k$ are currently active, then these k nodes tend to recover independently and simultaneously. Since γ_{i_l} is the instantaneous recovery rate of i_l for $l = 1, \ldots, k$, i.e. the time for node i_l to recovery follows $\exp(\gamma_{i_l})$ distribution, we know the instantaneous recovery rate of combination $\{i_1, \ldots, i_k\}$ is $\sum_{l=1}^{k} \gamma_{i_l}$ by Proposition 2.1. According to Lemma 2.1, the overall instantaneous recovery rate r_k for G to transfer from M_k to M_{k-1} is given by (22).

Besides recovery of nodes $i_1, \ldots, i_k$, the remaining inactive nodes also tend to be self-activated. In other words, there are $K - k$ independent and simultaneous self-activation processes at the inactive nodes $\{j : j \neq i_l, l = 1, \ldots, k\}$. The time for self-activation of inactive node j follows distribution $\exp(\beta_j)$ independently, and hence the total instantaneous self-activation rate of these $K - k$ nodes is $\sum_{j\neq i_l,\forall l} \beta_j$ by Proposition 2.1.

Finally, an active nodes i_l also tend to activate their inactive children in set $C_{i_l} \setminus \{i_1, \ldots, i_k\}$ independently and simultaneously. Therefore, the instantaneous rate for node i_l to perform a node-to-node activation is $\sum_{j\in C_{i_l}\setminus\{i_1,\ldots,i_k\}} \alpha_{i_l,j}$, and hence the combined instantaneous hazard rate (for node-to-node activation) of nodes $i_1, \ldots, i_k$ is given by $\alpha(i_1, \ldots, i_k)$ in (23) according to Proposition 2.1. Therefore, the overall instantaneous hazard rate q_k for G to transfer from metastate M_k to M_{k+1} is given by (21) according to Lemma 2.1. □

Theorem 2.1 provides a clear interpretation of the instantaneous rates q_k and r_k: they can be thought of as a convex combination of specific hazard and recovery rates generated by the $\binom{K}{k}$ combinations with $\mathrm{P}(t; i_1, \ldots, i_k)$ as the weights. Although it is not practical to obtain the (relative) probabilities of all $\binom{K}{k}$ combinations in general, we can develop several methods to estimate q_k and r_k with much lower computational cost by exploiting the probability weights. In what follows, we provide three methods for such estimation.

2.3.1 Shortest distance

In a large number of propagation network applications, the nodes cannot be self-activated or recover, which essentially yields a susceptible-infection (SI) propagation model. In this case $\beta_i = \gamma_i = 0$ for all nodes i, and hence we obtain $r_k = 0$ and

$$q_k(t) = \sum_{(i_1,\dots,i_k)\subset V} \alpha(i_1,\dots,i_k)\,\mathrm{P}(t; i_1,\dots,i_k), \tag{24}$$

where $\alpha(i_1,\dots,i_k)$ is defined in (23), according to Theorem 2.1. As a coarse but very low-cost approximation, we use only the combination with the dominating probability to estimate q_k. That is, suppose combination $\{i_1,\dots,i_k\}$ has the largest probability $\mathrm{P}(t; i_1,\dots,i_k)$ among all combinations of k nodes, then we set $q_k = \alpha(i_1,\dots,i_k)$ as given in (23). Now the remaining question is how to find the combination with the dominating probability.

Recall that the expected time for node i to activate its child j is $1/\alpha_{i,j}$, so it is natural to define the distance from i to j as $1/\alpha_{i,j}$. This distance can be easily generalized to any two nodes on the graph, and hence to a node and a set of nodes. we can easily see that the combination of k nodes of shortest distance to S has the dominating probability among all combinations due to the independency between all activation processes and memoryless property of exponential distributions.

In summary, we obtain $q_k(t)$ in the following way: let the indices of nodes with ascending distance to source S be $i_1, i_2, \dots, i_K$ (if $i \in S$ then the distance from i to S is 0) using Dijkstra's method [55], then we set

$$q_k(t) = \alpha(i_1,\dots,i_k), \quad \text{for } k = 1,\dots,K-1. \tag{25}$$

We note that in this setting the rate remains constant once the source set S is given. This method is referred to as `FPE-dist` in the numerical experiments.

Despite its simplicity, the estimate using shortest distance between nodes and source set is shown to be very efficient and accurate when compared to recently developed methods in many tests, as shown in our numerical experiments in Section 3. However, we point out this estimate is rather coarse and may fail in a number of cases. For instance, consider a network G where node i has two children j and k as shown in (26). The arrows show the edges and the numbers above indicate the activation rates.

$$\cdots \xleftarrow{1} j \xleftarrow{1} i \xrightarrow{1-\epsilon} l \xrightarrow{10^3} \cdots \tag{26}$$

Suppose now that node i is the source. Then even for $0 < \epsilon \ll 1$, the shortest distance method yields an estimate $q_2 = 2 - \epsilon \approx 2$, whereas according to Theorem 2.1 the rate should rather be $q_2 = \frac{1}{2-\epsilon} + \frac{1-\epsilon}{2-\epsilon} \cdot 10^3 \approx \frac{10^3}{2} \gg 2$. This issue can be amended by using multiple dominating combinations, as shown in the following method.

2.3.2 Truncation

In the same setting of SI propagation as above, a finer and more accurate estimate of the instantaneous rate (21) can be adopted to find multiple dominating combinations with largest probabilities (shortest distance method above finds only the one with the largest probability). We explain this method in a recursive fashion. Suppose that we already obtained m combinations of k nodes with dominating probabilities, denoted by $\{(i_1^{(l)},\dots,i_k^{(l)}) : l = 1,\dots,m\}$ with descending probabilities

$\mathrm{P}(i_1^{(l)}, \ldots, i_k^{(l)})$ as $l = 1, \ldots, m$. Then for $(i_1^{(l)}, \ldots, i_k^{(l)})$, the probability of activating a specific $j \in \cup_{s=1}^{k} C_{i_s{}^{(l)}} \setminus \{i_1^{(l)}, \ldots, i_k^{(l)}\}$, i.e., a specific inactive neighbor of them, is

$$\mathrm{P}(j|i_1^{(l)}, \ldots, i_k^{(l)}) = \frac{\sum_{s: j \in C_{i_s{}^{(l)}} \setminus \{i_1^{(l)}, \ldots, i_k^{(l)}\}} \alpha_{i_s^{(l)}, j}}{\sum_{s=1}^{k} \sum_{j' \in C_{i_s{}^{(l)}} \setminus \{i_1^{(l)}, \ldots, i_k^{(l)}\}} \alpha_{i_s^{(l)}, j'}}. \tag{27}$$

Note that the probability of combination $(j, i_1^{(l)}, \ldots, i_k^{(l)})$ where j is activated later than all $\{i_s^{(l)} : 1 \le s \le k\}$ is

$$\mathrm{P}(j, i_1^{(l)}, \ldots, i_k^{(l)}) = \mathrm{P}(j|i_1^{(l)}, \ldots, i_k^{(l)})\, \mathrm{P}(i_1^{(l)}, \ldots, i_k^{(l)}) \tag{28}$$

Once finished computing these probabilities for all inactive neighbors of $i_1^{(l)}, \ldots, i_k^{(l)}$, we sort them in descending order. As we proceed with $l = 1, \ldots, m$ in order, if we find a combination $(j, i_1^{(l)}, \ldots, i_k^{(l)})$ coincide with one found earlier $(j', i_1^{(l')}, \ldots, i_k^{(l')})$, then we merge their probabilities and remove $(j, i_1^{(l)}, \ldots, i_k^{(l)})$ from the next round. Through this process, we are likely (but not guaranteed) to keep the most dominating combinations. Note that this process again returns constant combination probabilities and hence constant q_k in (21).

This method essentially constructs a tree where each node has a relative probability and represents a specific combination of nodes in the propagation network being active, and the tree nodes with sufficiently small probabilities in a propagation are removed so that computation complexity is maintained under a feasible level. We refer this method as `FPE-tree` in the numerical experiments.

2.3.3 Most probably active nodes

The two methods above provide heuristic and simple estimation of instantaneous hazard rate for non-self-activation and non-recovery scenario. In the presence of recovery (still assuming non-self-activation as it is trivial to add this feature later), the k active nodes may scatter on the network at any moment. In this case, we need to estimate the probability which nodes are likely to be active, and use this to compute the combined hazard rate. In this work, we can adopt the method called N-interwined mean field approximation (NIMFA) in [58] to approximate the probability $p_i(t)$ of each node i being active at time t. More precisely, the `NIMFA` method estimates the probability $p_i(t)$ by solving the system of nonlinear differential equations:

$$p_i'(t) = \sum_{j \in D_i} \alpha_{j,i}(1 - p_i(t))p_j(t) - \gamma_i p_i(t), \tag{29}$$

for $i = 1, \ldots, K$. The approximation lies in the replacement of unknown joint distribution $p_{ij}(t)$, i.e. probability that both i and j are active at time t, by the product of $p_i(t)$ and $p_j(t)$ [58] for neighbors i and j. This replacement implicitly assumes independency of neighbor nodes i and j being active, which is obviously biased. However, if we do not adopt such replacement, then we need to establish additional differential equations for joint distribution $p_{ij}(t)$, and from there, joint distributions of $p_{ijk}(t)$ (probability that i, j and k are active at time t) etc. Eventually, the system of differential equations will reach size of order 2^K where all joint distributions up to $p_{1\cdots K}(t)$ are included, which is again intractable. It is possible that we terminate such increase of system dimension at some degree (NIMFA terminates at first degree where $p_{ij}(t)$ is replaced by $p_i(t)p_j(t)$), which may yield a moderate size of system with more accurate solution than `NIMFA`, however, it is beyond the scope of this paper.

Suppose that we have solved the system (29), from which we obtained approximation of probability $p_i(t)$ that a node i is active at time t. Now we can order the nodes with descending probability as $i_1(t), i_2(t), \ldots, i_K(t)$, i.e. $p_{i_1(t)}(t) \geq p_{i_2(t)}(t) \geq \cdots \geq p_{i_K(t)}(t)$, at any given time t. That is, we know which nodes are more likely to be active than others at time t. Then we set $q_k(t)$ to

$$q_k(t) = \alpha(i_1(t), \ldots, i_k(t)) + \sum_{j \neq i_l(t), \forall l} \beta_j, \tag{30}$$

and the instantaneous recovery rate $r_k(t)$ as

$$r_k(t) = \sum_{l=1}^{k} \gamma_{i_l(t)}. \tag{31}$$

Note that in this case the generator matrix $Q(t)$ depends on t.

2.4 Solution of the Fokker-Planck equation

Once we obtained the estimated q_k and r_k, the last step is to solve the Fokker-Planck equation (14) efficiently. According to the special structure of (14), we provide two means that compute the solution with very low complexity.

For the case of constant Q, a direct method is to apply matrix exponential and obtain $\rho(t) = \rho(0)e^{tQ}$ for any given t. The matrix exponential can be computed very efficiently since Q is merely a tridiagonal matrix [44, 54, 65]. In the case of time-varying Q or Q is very large, one can apply Runge-Kutta method to solve the system (14) efficiently. The advantage of using Runge-Kutta method is that it can handle more complicated generator matrix Q, such as time-varying and ρ-dependent Q. The drawback is that the computation of $\rho(t)$ needs to be proceeded from time 0 to t in proper time step increments.

2.5 Summary of solution steps and computational complexity

The solution of the proposed method consists of two phases: (i) obtaining the rates q_k and r_k in transition matrix Q, and (ii) computing the solution of $\rho'(t) = \rho(t)Q(t)$ numerically. The phase (i) can be accomplished in different ways according to propagation property and accuracy requirement as shown in Section 2.3. For instance, if Dijkstra's algorithm is employed in the first part, the complexity is at most $O(|E| + K \log K)$. Note that the output of Dijkstra's algorithm can be reused for computing influence of different source sets. If we employ the `NIMFA` algorithm to obtain q_k and r_k, then the complexity is to solve a system of K nonlinear differential equations with required step size, whose complexity is even lower than the Dijkstra's method. For other method to estimate q_k and r_k, the complexity depends on the structure of network G and may increase quickly as the density (average out degree) increases.

The computation to solve the Fokker-Planck equation numerically in phase (ii) has a fixed level of complexity regardless of the density of network structure. In this part, we need to solve a system of differential equations $\rho'(t) = \rho(t)Q(t)$ where $Q(t)$ is tridiagonal (bidiagonal without recovery) at any time t. Therefore, either matrix exponential or Runge-Kutta method to solve the system requires low complexity in terms of network size K. For instance, the complexity of Runge-Kutta method for solving this system is $O(K)$. In the next section, we performed several tests and measured the CPU time (in seconds) on a variety of network sizes up to $K = 10^8$. For benchmark

reference, we implemented the algorithm using MATLAB R2015a (64-bit) on a regular desktop computer equipped with Intel Core i7-3770 3.4GHz CPU (only single core is used in computation) and 32GB of memory. The CPU time is shown in the left panel of Figure 4. In particular, the total CPU time, including estimation of rate matrix Q using Dijkstra's method and solving system of equations using 4th order Runge-Kutta method, to predict influence up to $T = 10$ is 0.3 second for the example of Kronecker network of size $K = 1,024$ and average out degree 1.56 in left panel of Figure 4 (with only minor increase of cost in estimating rates using Dijkstra's method for dense Erdős-Rényi's random network and small-world network). In contrast, the `ConTinEst` applied to the sparse Kronecker network is reported to take nearly 4 seconds on powerful parallel computer cluster with 192 cores of 2.4GHz, where the computational cost can drastically increase further if the network becomes dense.

3 Experimental results

In this section, we demonstrate the performance of the proposed method using propagation networks with various size, density, and topology. For the purpose of comparison, we also evaluate several recently developed algorithms for influence prediction. As these algorithms have different assumptions on propagation models and input data format, we separate the experimental settings to be suitable for each of these comparison algorithms.

3.1 Common settings in the experiments

In the numerical tests, we simulate a variety of network structures with different size and degree distributions. In particular, we construct the Erdős-Rényi's random graph, small-world network, scale-free network using the `CONTEST` package [56], and Kronecker network in the `ConTinEst` code [15]. The size and degree distribution will be presented along with the experiments later. For the Erdős-Rényi's random graph, small-world network, and scale-free network, the activation rates $\{\alpha_{ij} : (i, j) \in E\}$ are drawn from continuous Uniform(0,1) distribution independently (using MATLAB built-in `rand` function) to simulate the inhomogeneous propagation rates between different nodes. These rates for the Kronecker network are obtained directly from the Kronecker network data in `ConTinEst` code. Note that the Kronecker network is very sparse for `ConTinEst` to be computationally feasible as it in general requires extensive amount of samplings.

In each test, a prescribed number of source nodes are randomly selected from the network, except the one in the middle panel of Figure 4 which is to show the impact of different source nodes on the influence. Given the network $G(V, E)$, activation rates $\alpha_{i,j}$ and recovery rates γ_i, and identities of source nodes, we use Monte Carlo Markov chain (MCMC) to simulate $5,000$ propagations. Then the reference is set to the averaged influence of these propagations in the corresponding test.

3.2 Numerical results and evaluations

3.2.1 Tests on homogeneous complete graphs

The first test is to verify the exactness of solution on influence prediction by FPE on complete graph with SIS propagation model. In this test, we use constant node-to-node activation rate $\alpha = 1$ and recovery rate $\gamma = \tau\|A\|_2$ for three different values of $\tau = 10$, 1.1, and 0.1 respectively. For comparison purpose, we also implemented the `NIMFA` method [58, 59] which is based on mean-field

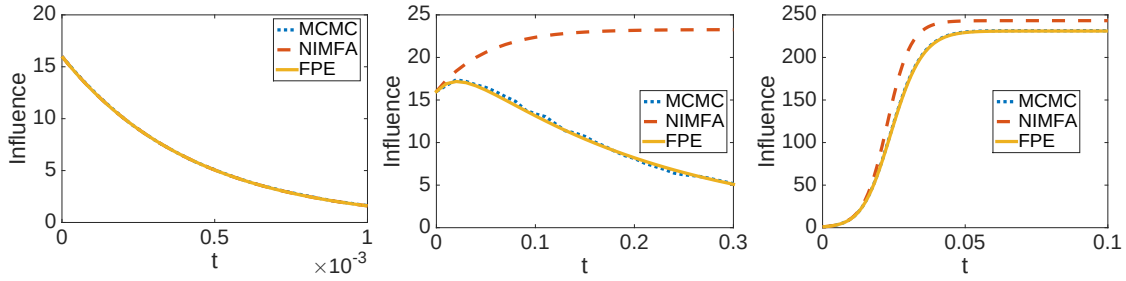

Figure 1: Influence prediction on complete graph of size $K = 256$ where the activation rate $\alpha = 1$ and recovery rate $\gamma = 255\tau$ with τ set to 10 (left), 1.1 (middle), and 0.1 (right).

approximation theory. In Figure 1, we show the evolving influence estimated by `NIMFA` (29) and the proposed method shown in (10) on complete graph of sizes $K = 256$ with different ratio of γ/α. Note that the threshold ratio is $\|A\|_2 = \|A\|_\infty = K - 1$ in this case. The solution of Fokker-Planck equation (10), in yellow solid line, is exact from our earlier theoretical analysis, and shows here to matches the MCMC simulation in blue dotted line. In contrast, the estimation `NIMFA` shown by red dashed line deviates significantly from the true solution when $\gamma/\alpha = 1.1\|A\|_2$. Similar deviations phenomena of `NIMFA` is also reported in [59].

It is worth pointing out that this numerical test on complete graph is just to verify the correctness of the new Fokker-Planck equation approach. In this special case, the network is homogenous and the nodes are equivalent (hence identities of source nodes make no difference either), and therefore certain methods in statistical physics, such as approximate mater equation (AME) [21], can also be applied and yield accurate solution. In the remaining part of this section, we only consider the heterogeneous networks which have given structure and nonuniform activation rates $\alpha_{i,j}$, and the identities of source nodes have impact on the influence prediction.

3.2.2 Tests on general heterogeneous networks

Our remaining tests are carried out on various networks without recovery scenario, i.e., using the SI propagation model. As for now, the Fokker-Planck equation based approach with truncated probability tree estimation for transition rate (`FPE-tree`) given in Section 2.3.2 is not scalable for large networks in general, we only test it on small networks. In Figure 2, we showed the performance of the FPE based approach using shortest distance estimation (`FPE-dist`) given in Section 2.3.1 and `FPE-tree` on a random Erdős-Rényi's network of size 16, of size 32, and a small-world network of size 32, all with an average node (out)degree 4. The FPE based approaches appear to be very accurate compared to mean-field approximation based approach.

Note that the `FPE-dist` method in Section 2.3.1 has very low computational cost, we test it on networks of larges sizes and various connectivities. In Figure 3, we show the influence prediction result for Erdős-Rényi's network (left), small-world network (middle), and scale-free network (right) of size $K = 1,024$ and average node (out)degree 8, 6, and 6 respectively. Despite of difference in network structure, results by `FPE-dist` show faithful influence prediction and matches MCMC simulations closely.

Since the influence prediction problem is considered computationally very challenging especially for dense heterogeneous networks, we test `FPE-dist` for Erdős-Rényi's random network with much

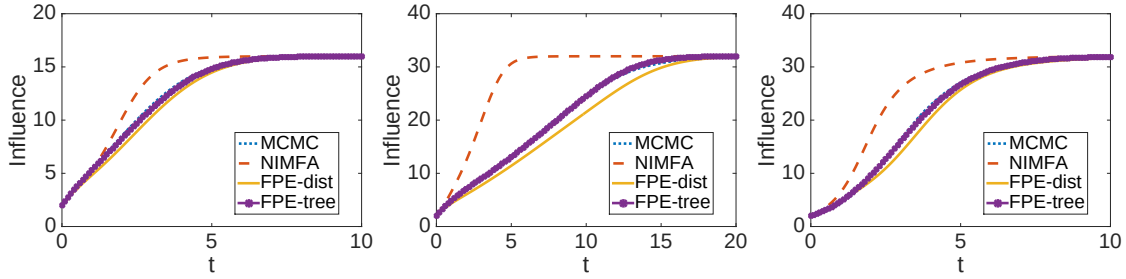

Figure 2: Influence prediction on small networks with SI model. Left: Erdős-Rényi's network of size 16. Middle: Erdős-Rényi's network of size 32. Right: Small-world network of size 32. All networks have average node (out)degree 4. The activation rates $\alpha_{i,j}$ are drawn randomly from continuous Uniform(0,1) distribution.

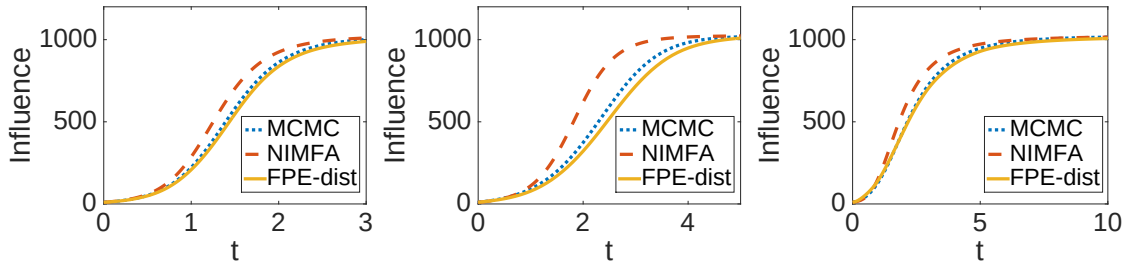

Figure 3: Influence prediction on Erdős-Rényi's network (left), small-world network (middle), and scale-free network (right) of size $K = 1024$ using SI propagation model. Average node (out)degree is set to 8, 6, and 6 respectively. The activation rates $\alpha_{i,j}$ are drawn randomly from continuous Uniform(0,1) distribution.

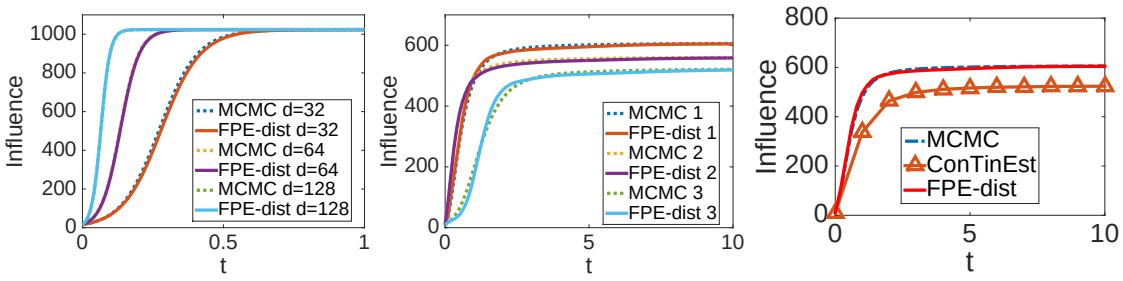

Figure 4: Left: influence prediction on Erdős-Rényi's random network of size $K = 1,024$ and three different average node (out)degree $d = 32, 64, 128$. Middle: influence prediction using three different combinations of 10 source nodes on the same Kronecker network of size $1,024$. Right: comparison with `ConTinEst` on influence prediction using its included Kronecker network.

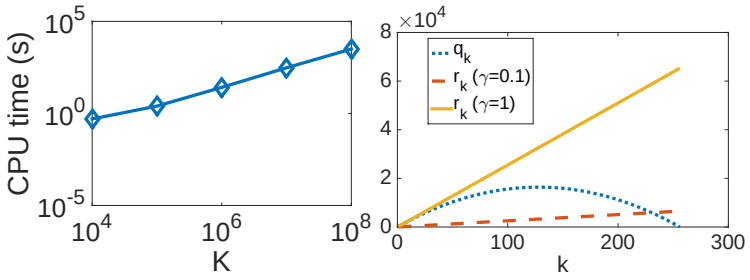

Figure 5: Left: CPU time (in seconds) of `FPE-dist` using Runge-Kutta 4th order ODE solver on networks of different sizes K. Right: The transition rates q_k and r_k (for recovery rate $\gamma = 0.1$ and 1) in (10) for $k = 1, 2, \ldots, K$ in the complete graph (size $K = 256$) example.

dense configuration (high node degree). In the left panel of Figure 4, we generate three random networks of size $K = 1,024$ and average node (out)degree $d = 32$, 64, and 128 respectively. On all of these networks, `FPE-dist` returns highly accurate prediction of influence which justifies its robustness.

As we pointed out earlier, the influence prediction problem in this paper is significantly different from those in the study of dynamical processes on networks in statistical physics: the network structure and activation rates between nodes are heterogeneous and already fixed. The goal is to efficiently calculate the influence of given source nodes. Therefore, the influence depends on the identities of the source nodes. In the middle panel of Figure 4, we use a Kronecker network of size $K = 1,024$ and average node (out)degree 1.56 from the `ConTinEst` code with three different sets of source nodes. In the first set, we use the 10 nodes selected by the built-in greedy influence maximization subroutine of `ConTinEst`; in the second set, we select the 10 nodes of largest (out)degree in the network; and in the last set, we randomly select 10 nodes from the network. It can be seen that `FPE-dist` is robust in all cases. More importantly, the plots clearly show that the identities of source nodes who initialize the propagation play an important role in the influence prediction problem.

We also compared `FPE-dist` to the recently developed `ConTinEst` algorithm [15]. `ConTinEst`

is a learning-based algorithm that uses kernel functions to approximate the coverage of each node based on Monte-Carlo samplings. `ConTinEst` also requires network structure, propagation model and parameters, but can be applied to any transmission distribution (not necessarily exponential) as long as the activation on all edges are independent (essentially the independent cascade model). However, `ConTinEst` cannot handle the case with recovery scenario as the coverage function cannot be learned from cascades in straightforward manner. In addition, `ConTinEst` can only estimate influence for a prescribed time but not the temporal changes. To obtain the estimate for multiple time points we need to rerun `ConTinEst` for each time. The performance is shown in the right panel of Figure 4. In our test, we directly employ the `ConTinEst` code published online by the authors and input a network with exponential distributed transmission parameters. From this test, we see that `FPE-dist` is very accurate as it matches the MCMC simulations much better.

Note that comprehensive comparison of `ConTinEst` with several other existing state-of-the-arts methods is also reported in [15], from which significant improvement in accuracy of the proposed method `FPE-dist` can be projected by comparing with `ConTinEst` in the right panel of Figure 4. Therefore, the proposed method is potentially a much more efficient and accurate subroutine to calculate time evolving influence of given source set, and hence makes influence maximization [10, 28, 31, 61] or outbreak detection [11, 37] result more reliable.

As we have showed earlier, the proposed method possesses low computation complexity and is scalable for large and dense networks. In particular, the computational time to solve the system of equations for different scales of dense network is shown in the left panel of Figure 5, which indicates the high efficiency of the proposed method. In contrast, most state-of-the-arts sampling-based approaches suffer drastic increase of computational cost for larger or denser networks due to the significantly amplified number of simulations required to achieve acceptable level of accuracy.

4 Conclusion and open questions

In this paper, we consider the influence prediction problem on general heterogeneous network. Given a network (directed graph) $G(V, E)$, the activation rates $\{\alpha_{i,j} : (i, j) \in E\}$ (and self-activation rates $\{\beta_i : i \in V\}$ and recovery rates $\{\gamma_i : i \in V\}$ if the corresponding scenarios are considered), and the source set S of initially active nodes, we want to effectively estimate the influence $\mu(t; S)$ defined by the expected number of active nodes at time t.

We establish a system of ordinary differential equations which governs the probability mass functions on the state graph where each node lumps a number of activation states of G. Such a system is constructed on a discrete space (the state graph), and can be thought of as an analogue of the Fokker-Planck equations for stochastic processes in continuous spaces. We provide several methods to estimate the system parameters in terms of the given source set S and rates $\{\alpha_{i,j} : (i, j) \in E\}$ etc. Numerical experiments show that the proposed methods are very efficient and accurate to solve the influence prediction problem, which is considered very challenging computationally in the literature.

Our approach gives rise to a novel framework that can effectively solve the influence prediction problem on large-scale, complex, and heterogeneous networks. This framework is established on the lumped state graph where the nodes each represents a different value of $N(t; S)$. It has a great potential to deal with general propagation models, and also opens a number of interesting questions. For example:

1. What if the the propagation model is not exponential? For instance, if the random activation

times each follows a Weibull or Hawkes distribution, will the proposed strategies still work? Can we find ways to estimate the transition rates q_k and r_k accurately and efficiently?

2. In real-world problems, the network structure and/or propagation models are often unknown or only partially known. What and how to learn the transition rates from data directly?

3. Based on Theorem 2.1, can we obtain tight error bounds for the parameter estimation, and hence establish a comprehensive and practically useful error analysis of the proposed framework?

These problems are obviously challenging, and they are included in our research plan. We hope to report our findings in the future.

Appendix

We continue the discussion on the classical SIS model on complete graphs in Section 2.1. In particular, we explore the eigenvalue structure of Q and its relation to the stationary distribution of propagation. Note that the solution (13) by the proposed method not only yields an efficient way to estimate the influence, but also provides some insights of the asymptotic properties of the propagation in terms of the node-to-node activation rate α, self-activation rate β, and recovery rate γ. More precisely, we observe that

1. If $\gamma = 0$ and $\beta = 0$, then the matrix Q is bidiagonal and the transition rates $Q_{k,k+1} = k(K-k)\alpha$. Hence the expected time for the a new node getting activated in a network with k active nodes is $1/k(K-k)\alpha$. Therefore, if there are $|S|$ nodes active initially, then the expected time for all nodes to get activated is

$$\sum_{k=|S|}^{K-1} \frac{1}{k(K-k)\alpha} = \frac{2}{K\alpha} \sum_{k=|S|}^{K-1} \frac{1}{k} \approx \frac{2}{\alpha} \left(\frac{\log K}{K} - \frac{\log |S|}{|S|} \right) \tag{32}$$

   In particular, if there is one node initially active, then the expected time for all nodes in the complete graph of size K to get activated is approximately $2 \log K/(K\alpha)$.

2. If $\gamma = 0$, the system (13) with matrix Q in (12) exhibits one absorbing state at $(0, \ldots, 0, 1)$ for any initial value $\rho(0)$ for $\alpha > 0$ (and $\rho(0) \neq (1, 0, \ldots, 0)$ for $\alpha = 0$). Namely, all nodes will eventually get activated as long as there is self-activation, or there is no self-activation but at least one node is active initially.

3. If $\gamma > 0$ and $\beta = 0$, the system exhibits one absorbing state at $(1, 0, \ldots, 0)$, meaning that all nodes will eventually be recovered. However, there exists a metastable state that the network has a certain fraction of nodes being active for extended long period, as also noted in [59].

4. If $\gamma > 0$ and $\beta > 0$, there is one steady state of the system that associates to the 0 eigenvalue of matrix Q given in (12). In particular $N(t; S)$, the number of active nodes in network G, converges to a stationary distribution $\rho^* = (\rho_0^*, \ldots, \rho_K^*)$ where

$$\rho_0^* = \left(1 + \sum_{k=1}^{K} \prod_{i=1}^{k} \frac{Q_{i-1,i}}{Q_{i,i-1}} \right)^{-1} \text{ and } \rho_k^* = \rho_0^* \cdot \left(\prod_{i=1}^{k} \frac{Q_{i-1,i}}{Q_{i,i-1}} \right), \tag{33}$$

   for $k = 1, \ldots, K$ and is independent of the size of S.

5. We set $\alpha = 1$, $\beta = 0$, and change γ to test how the ratio α/γ affects the propagation. Note that now $q_k = k(K-k)$ (blue dotted) and $r_k = k\|A\|_2\gamma$, as shown in Figure 5 for $K = 256$, where $\|A\|_2 = K-1$ for complete graph. If $\gamma = 1$ (yellow solid), which is the threshold value, there are $r_1 = q_1$ and $q_k < r_k$ for all $k = 2, \ldots, K-1$. If $\gamma < 1$ (red dashed), then the lines of q_k and r_k intersect near some $k_0 > 1$ and the initial state may affect the behavior of influence evolution. Empirically, varying ratios yield different patterns of influence as shown in Figure 1.

The properties listed above are direct consequences from the eigenvalue system or the structure of Q. We expect that more important properties can be obtained by this new approach, and that such analysis framework can be extended to general propagation networks.

References

[1] R. Albert and A.-L. Barabási. Statistical mechanics of complex networks. *Reviews of modern physics*, 74(1):47, 2002.

[2] R. M. Anderson, R. M. May, and B. Anderson. *Infectious diseases of humans: dynamics and control*, volume 28. Wiley Online Library, 1992.

[3] G. Bianconi and A.-L. Barabási. Competition and multiscaling in evolving networks. *EPL (Europhysics Letters)*, 54(4):436, 2001.

[4] S. Boccaletti, G. Bianconi, R. Criado, C. I. Del Genio, J. Gómez-Gardeñes, M. Romance, I. Sendiña-Nadal, Z. Wang, and M. Zanin. The structure and dynamics of multilayer networks. *Physics Reports*, 544(1):1–122, 2014.

[5] M. Boguná and R. Pastor-Satorras. Epidemic spreading in correlated complex networks. *Physical Review E*, 66(4):047104, 2002.

[6] B. Bollobás. *Random graphs*. Springer, 1998.

[7] C. Castellano, S. Fortunato, and V. Loreto. Statistical physics of social dynamics. *Reviews of modern physics*, 81(2):591, 2009.

[8] K. Choromański, M. Matuszak, and J. Mi kisz. Scale-free graph with preferential attachment and evolving internal vertex structure. *Journal of Statistical Physics*, 151(6):1175–1183, 2013.

[9] S.-N. Chow, W. Huang, Y. Li, and H. Zhou. Fokker–planck equations for a free energy functional or markov process on a graph. *Archive for Rational Mechanics and Analysis*, pages 1–40, 2011.

[10] E. Cohen, D. Delling, T. Pajor, and R. F. Werneck. Timed influence: Computation and maximization. *arXiv preprint arXiv:1410.6976*, 2014.

[11] P. Cui, S. Jin, L. Yu, F. Wang, W. Zhu, and S. Yang. Cascading outbreak prediction in networks: a data-driven approach. In *Proceedings of the 19th ACM SIGKDD international conference on Knowledge discovery and data mining*, pages 901–909. ACM, 2013.

[12] G. Demirel, F. Vazquez, G. Böhme, and T. Gross. Moment-closure approximations for discrete adaptive networks. *Physica D: Nonlinear Phenomena*, 267:68–80, 2014.

[13] S. N. Dorogovtsev. *Lectures on complex networks*, volume 24. Oxford University Press Oxford, 2010.

[14] N. Du, Y. Liang, M.-F. Balcan, and L. Song. Influence function learning in information diffusion networks. In *International Conference on Machine Learning*, 2014.

[15] N. Du, L. Song, M. Gomez-Rodriguez, and H. Zha. Scalable influence estimation in continuous-time diffusion networks. In *Advances in Neural Information Processing Systems*, page to appear, 2013.

[16] R. Durrett. *Lecture notes on particle systems and percolation*. Wadsworth & Brooks/Cole Advanced Books & Software, 1988.

[17] R. Durrett. *Random graph dynamics*, volume 200. Cambridge University Press, 2007.

[18] P. Erdös and A. Rényi. On random graphs i. *Publ. Math. Debrecen*, 6:290–297, 1959.

[19] J. Friedman. Individual strategy and social structure., 1998.

[20] E. N. Gilbert. Random graphs. *The Annals of Mathematical Statistics*, pages 1141–1144, 1959.

[21] J. P. Gleeson. High-accuracy approximation of binary-state dynamics on networks. *Physical Review Letters*, 107(6):068701, 2011.

[22] J. P. Gleeson. Binary-state dynamics on complex networks: Pair approximation and beyond. *Physical Review X*, 3(2):021004, 2013.

[23] J. Goldenberg, B. Libai, and E. Muller. Talk of the network: A complex systems look at the underlying process of word-of-mouth. *Marketing letters*, 12(3):211–223, 2001.

[24] J. Goldenberg, B. Libai, and E. Muller. Using complex systems analysis to advance marketing theory development: Modeling heterogeneity effects on new product growth through stochastic cellular automata. *Academy of Marketing Science Review*, 9(3):1–18, 2001.

[25] M. Gomez-Rodriguez, D. Balduzzi, and B. Schölkopf. Uncovering the temporal dynamics of diffusion networks. *arXiv preprint arXiv:1105.0697*, 2011.

[26] M. Gomez-Rodriguez, J. Leskovec, and A. Krause. Inferring networks of diffusion and influence. *ACM Transactions on Knowledge Discovery from Data (TKDD)*, 5(4):21, 2012.

[27] M. Gomez-Rodriguez, J. Leskovec, and B. Schölkopf. Modeling information propagation with survival theory. In *Proceedings of the 30th International Conference on Machine Learning (ICML-13)*, pages 666–674, 2013.

[28] M. Gomez Rodriguez, B. Schölkopf, L. J. Pineau, et al. Influence maximization in continuous time diffusion networks. In *29th International Conference on Machine Learning (ICML 2012)*, pages 1–8. International Machine Learning Society, 2012.

[29] M. Granovetter. Threshold models of collective behavior. *American journal of sociology*, pages 1420–1443, 1978.

[30] M. O. Jackson. *Social and economic networks*, volume 3. Princeton University Press Princeton, 2008.

[31] D. Kempe, J. Kleinberg, and É. Tardos. Maximizing the spread of influence through a social network. In *Proceedings of the ninth ACM SIGKDD international conference on Knowledge discovery and data mining*, pages 137–146. ACM, 2003.

[32] J. O. Kephart and S. R. White. Directed-graph epidemiological models of computer viruses. In *Research in Security and Privacy, 1991. Proceedings., 1991 IEEE Computer Society Symposium on*, pages 343–359. IEEE, 1991.

[33] E. D. Kolaczyk and G. Csárdi. *Statistical analysis of network data with R*. Springer, 2014.

[34] V. G. Kulkarni. Shortest paths in networks with exponentially distributed arc lengths. *Networks*, 16(3):255–274, 1986.

[35] J. Leskovec, L. A. Adamic, and B. A. Huberman. The dynamics of viral marketing. *ACM Transactions on the Web (TWEB)*, 1(1):5, 2007.

[36] J. Leskovec, L. Backstrom, and J. Kleinberg. Meme-tracking and the dynamics of the news cycle. In *Proceedings of the 15th ACM SIGKDD international conference on Knowledge discovery and data mining*, pages 497–506. ACM, 2009.

[37] J. Leskovec, A. Krause, C. Guestrin, C. Faloutsos, J. VanBriesen, and N. Glance. Cost-effective outbreak detection in networks. In *Proceedings of the 13th ACM SIGKDD international conference on Knowledge discovery and data mining*, pages 420–429. ACM, 2007.

[38] T. M. Liggett. *Interacting particle systems*. Springer, 2005.

[39] J. Lindquist, J. Ma, P. Van den Driessche, and F. H. Willeboordse. Effective degree network disease models. *Journal of mathematical biology*, 62(2):143–164, 2011.

[40] M. W. Macy. Chains of cooperation: Threshold effects in collective action. *American Sociological Review*, pages 730–747, 1991.

[41] M. W. Macy and R. Willer. From factors to actors: Computational sociology and agent-based modeling. *Annual review of sociology*, pages 143–166, 2002.

[42] V. Marceau, P.-A. Noël, L. Hébert-Dufresne, A. Allard, and L. J. Dubé. Adaptive networks: Coevolution of disease and topology. *Physical Review E*, 82(3):036116, 2010.

[43] J. C. Miller and I. Z. Kiss. Epidemic spread in networks: Existing methods and current challenges. *Mathematical modelling of natural phenomena*, 9(2):4, 2014.

[44] C. Moler and C. Van Loan. Nineteen dubious ways to compute the exponential of a matrix, twenty-five years later. *SIAM review*, 45(1):3–49, 2003.

[45] S. Morris. Contagion. *The Review of Economic Studies*, 67(1):57–78, 2000.

[46] M. Newman. *Networks: an introduction*. Oxford University Press, 2010.

[47] J.-P. Onnela, J. Saramäki, J. Hyvönen, G. Szabó, D. Lazer, K. Kaski, J. Kertész, and A.-L. Barabási. Structure and tie strengths in mobile communication networks. *Proceedings of the National Academy of Sciences*, 104(18):7332–7336, 2007.

[48] R. Pastor-Satorras, C. Castellano, P. Van Mieghem, and A. Vespignani. Epidemic processes in complex networks. *arXiv preprint arXiv:1408.2701*, 2014.

[49] D. Peleg. Local majority voting, small coalitions and controlling monopolies in graphs: A review. In *Proc. of 3rd Colloquium on Structural Information and Communication Complexity*, pages 152–169, 1997.

[50] M. A. Porter and J. P. Gleeson. Dynamical systems on networks: A tutorial. *arXiv preprint arXiv:1403.7663*, 2014.

[51] H. Ryu, M. Lease, and N. Woodward. Finding and exploring memes in social media. In *Proceedings of the 23rd ACM conference on Hypertext and social media*, pages 295–304. ACM, 2012.

[52] K. Saito, M. Kimura, K. Ohara, and H. Motoda. Learning continuous-time information diffusion model for social behavioral data analysis. In *Advances in Machine Learning*, pages 322–337. Springer, 2009.

[53] T. C. Schelling. *Micromotives and macrobehavior*. WW Norton & Company, 2006.

[54] R. B. Sidje. Expokit: a software package for computing matrix exponentials. *ACM Transactions on Mathematical Software (TOMS)*, 24(1):130–156, 1998.

[55] M. Sniedovich. Dijkstra's algorithm revisited: the dynamic programming connexion. *Control and cybernetics*, 35(3):599, 2006.

[56] A. Taylor and D. J. Higham. Contest: A controllable test matrix toolbox for matlab. *ACM Transactions on Mathematical Software (TOMS)*, 35(4):26, 2009.

[57] T. J. Taylor and I. Z. Kiss. Interdependency and hierarchy of exact and approximate epidemic models on networks. *Journal of mathematical biology*, 69(1):183–211, 2014.

[58] P. Van Mieghem and J. Omic. In-homogeneous virus spread in networks. *arXiv preprint arXiv:1306.2588*, 2013.

[59] P. Van Mieghem, J. Omic, and R. Kooij. Virus spread in networks. *Networking, IEEE/ACM Transactions on*, 17(1):1–14, 2009.

[60] A. Vespignani. Modelling dynamical processes in complex socio-technical systems. *Nature Physics*, 8(1):32–39, 2012.

[61] C. Wang, W. Chen, and Y. Wang. Scalable influence maximization for independent cascade model in large-scale social networks. *Data Mining and Knowledge Discovery*, 25:545–576, 2012.

[62] Y. Wang, D. Chakrabarti, C. Wang, and C. Faloutsos. Epidemic spreading in real networks: An eigenvalue viewpoint. In *Reliable Distributed Systems, 2003. Proceedings. 22nd International Symposium on*, pages 25–34. IEEE, 2003.

[63] D. J. Watts. A simple model of global cascades on random networks. *Proceedings of the National Academy of Sciences*, 99(9):5766–5771, 2002.

[64] D. J. Watts and S. H. Strogatz. Collective dynamics of small-world networks. *Nature*, 393(6684):440–442, 1998.

[65] J. Xue and Q. Ye. Computing exponentials of essentially non-negative matrices entrywise to high relative accuracy. *Mathematics of Computation*, 82(283):1577–1596, 2013.

[66] H. P. Young. The diffusion of innovations in social networks. *The Economy As an Evolving Complex System III: Current Perspectives and Future Directions*, 267, 2006.

[67] J. Zhang and J. M. Moura. Diffusion in social networks as sis epidemics: beyond full mixing and complete graphs. *Selected Topics in Signal Processing, IEEE Journal of*, 8(4):537–551, 2014.

[68] K. Zhou and H. Zha. Learning triggering kernels for multi-dimensional hawkes processes. In *International Conference on Machine Learning*, 2013.

[69] K. Zhou, H. Zha, and L. Song. Learning social infectivity in sparse low-rank networks using multi-dimensional hawkes processes. In *International Conference on Artificial Intelligence and Statistics (AISTATS)*, 2013.